Determination of the Binding of Ligands Containing the *N*-2,4-Dinitrophenyl Group to Bivalent Monoclonal Rat Anti-DNP Antibody Using Affinity Capillary Electrophoresis

Mathai Mammen, Frank A. Gomez,[†] and George M. Whitesides*

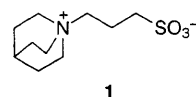*Department of Chemistry, Harvard University, 12 Oxford Street, Cambridge, Massachusetts 02138*

Affinity capillary electrophoresis has been used to determine the two dissociation constants of the complex between anti-DNP rat monoclonal IgG$_{2b}$ antibody and charged ligands that contained a *N*-dinitrophenyl group. Singly and multiply charged ligands were used to establish the influence of the charge on the mobility of the complex between Ig and its ligand(s). Zwitterionic buffer additives lessened adsorption of protein to the walls of the capillary. A form of analysis of the binding data is derived that is more useful than Scatchard analysis for certain multivalent systems where cooperativity of binding is in question, but where it is also possible to make plausible assumptions about electrophoretic mobilities of protein and protein−ligand complexes. The uncertainties and assumptions of this analysis are contrasted with those of Scatchard analysis. For this antibody and these monovalent ligands, the dissociation of the ligands from the antibody occurred noncooperatively. The charge on IgG$_{2b}$ at pH 8.3 is estimated to be -8.0 ± 0.2; this value is obtained by analysis of the electrophoretic mobilities of complexes IgG$_{2b}$L$_2$, where the ligands L are structurally similar but have different charges (the charges on the ligands were also determined by CE).

Nature uses polyvalency—the cooperative association of a receptor, or aggregate, having multiple recognition sites with a molecule containing multiple complementary ligands—to mediate many classes of biological interactions: between two surfaces (cell−cell,[1] cell−pathogen[2−4]); between a surface and a soluble species (cell−protein,[5] pathogen−protein,[6,7] pathogen−polysaccharide,[8] cell−polysaccharide[9]); and between two soluble species (protein−protein,[10] drug−ligand[11]). We wish to quantitate the contribution of simultaneous, multivalent binding to these interactions. As a first, preliminary step in developing analytical methods

applicable to polyvalent interactions, we have explored the use of affinity capillary electrophoresis (ACE)[12−15] to examine binding of *monovalent* ligands to *bivalent* antibodies. Polyvalent interactions can be either cooperative or noncooperative: the binding at one site may or may not influence binding at another site. We require methods applicable to cooperative systems and capable of yielding multiple dissociation constants. This study demonstrates a method for using ACE to extract dissociation constants of ligands from antibodies. It requires an assumption about the influence of binding of the ligand on the electrophoretic mobility of the protein and is, therefore, not completely general. This assumption, or its generalization, will, however, probably be met in many systems of interest. This system therefore models a common class of interactions involving an important class of proteins−immunoglobulins−that interact polyvalently.

We illustrate this method using ligands containing *N*-(2,4-dinitrophenyl)amino (DNP) groups and bivalent antibodies (rat myeloma monoclonal antibody, IgG$_{2b}$, hereafter referred to as Ig) that bind to DNP groups. These antibodies are well characterized and readily available.[16−18]

Proteins with high molecular mass (greater than ~50 kDa) and p*I* (greater than ~6.0) tend to give peaks on capillary electrophoresis under many conditions that are broad and unsymmetrical in shape (or to give no peaks at all) as a result of interactions with the wall of the capillary. The molecular mass of Ig is 150 kDa and its p*I* is 6.5; its peaks in simple buffers are broad. Use of zwitterionic additives to a simple buffer gives sharper, more symmetrical and highly reproducible peaks. We added 500 mM 3-quinuclidinopropanesulfonate (1) and 10 mM

1

K$_2$SO$_4$ to the buffer in all the experiments. This type of zwitterionic additive was originally proposed by Jorgenson.[19]

* Present address: California State University, Los Angeles, Department of Chemistry and Biochemistry, 5151 State University Drive, Los Angeles, CA 90032-8202.

(1) Cepek, K.; Brenner, M. B. *Nature* **1994**, *372*, 190.
(2) Sparks, M. A.; Williams, K. W.; Whitesides, G. M. *J. Med. Chem.* **1993**, *36*, 778−783.
(3) Cohen, J. A.; Williams, W. V. *Microbiol. Sci.* **1988**, *5*, 265−270.
(4) Collono, R. J. *Adv. Exp. Med. Biol.* **1992**, *312*, 61−70.
(5) Pantoliano, M. W.; Horlick, R. A. *Biochemistry* **1994**, *33*, 10229−10248.
(6) Roche, A. C.; Midoux, P. *Res. Virol.* **1990**, *141*, 243−249.
(7) Karlsson, K. A. *Trends Pharm. Sci.* **1991**, *12*, 265−272.
(8) Spear, P. G.; Shieh, M. T. *Adv. Exp. Med. Biol.* **1992**, *313*, 341−353.
(9) Mora-Perez, I.; Porres-Cubero, J. C. *Rev. Clin. Esp.* **1985**, *176*, 1−4.
(10) Dalgleish, A. G.; Kennedy, R. C. *Vaccine* **1988**, *6*, 215−220.
(11) Christian, B.; Waring, M. J. *Biochem. J.* **1994**, *300*, 165−173.

(12) Kuhr, W. G.; Monnig, C. A. *Anal. Chem.* **1992**, *64*, 389−407.
(13) Chu, Y. H.; Lees, W. J.; Stassinopoulos, A.; Walsh, C. T. *Biochemistry* **1994**, *33*, 10616−10621.
(14) Liu, J.; Volk, K. J.; Lee, M. S.; Kerns, E. H.; Rosenberg, I. E. *J. Chromatogr., A* **1994**, *680*, 395−403.
(15) Liu, J.; Volk, K. J.; Lee, M. S.; Pucci, M.; Handwerger, S. *Anal. Chem* **1994**, *66*, 2412−2416.
(16) Bazin, H. *Proteins and Biological Fluids, 29th Colloquium*; Pergamon Press: Oxford, U.K., 1982; pp 615−618.
(17) Kooistra, D. A.; Richards, J. H. *Biochemistry* **1978**, *17*, 345−351.
(18) Brunger, A. T.; Leahy, D. J.; Hynes, T. R.; Fox, R. O. *J. Mol. Biol.* **1991**, *221*, 239−256.
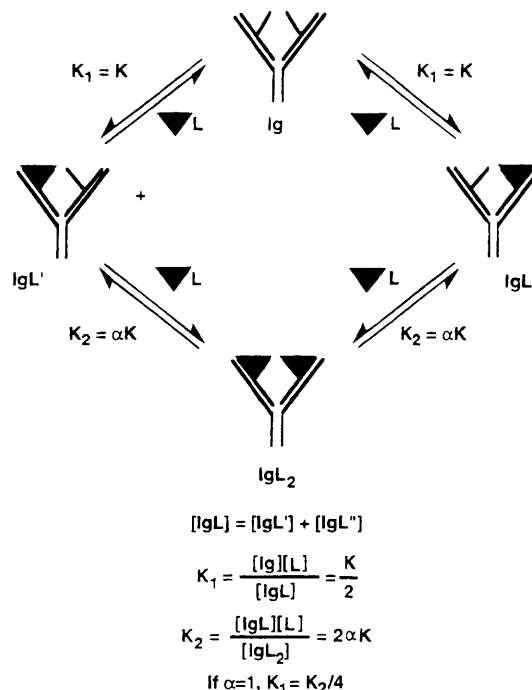
ACE yields dissociation constants by analysis of the change in electrophoretic mobility of a protein on binding a small charged ligand.[20,21] We derive these changes in electrophoretic mobility from changes in the time that the protein requires to reach the detector (the time of appearance, t_{app}) relative to the time required for several internal standards that are not influenced by the ligand. The change in the time of appearance (Δt_{app}) of a protein on binding a ligand must be greater than the width of its peak to be measured reliably. A typical width at half-height of the peaks in this study is ~10 s. The Δt_{app} is approximately proportional to the charge on the ligand, Z_L, and inversely proportional to the mass, M, of the protein (eq 1). Ig has a high molecular mass (150

$$\Delta t_{app} \propto Z_L/M^\alpha \qquad (1)$$

kDa). To achieve the required Δt_{app}, the value of Z_L for the ligand must therefore be relatively large. In this study, if $Z_L = -1$, Δt_{app} ~ 3 s; if $Z_L = -3$, Δt_{app} ~ 9 s. We synthesized and used ligands where $Z_L = -1$, -2, -3, and -9.

There have been several reports of positive cooperativity between the binding sites of antibodies that bind *monovalent* ligands, particularly for antibodies that bind DNP groups;[22-24] we could not, therefore, assume that binding of monovalent ligands to Ig occurred noncooperatively. Cooperativity would yield a curved plot in Scatchard analysis, and values for the two dissociation constants are not readily extracted from such a plot. Scatchard analysis, which was acceptable in mono-valent systems previously studied by ACE (e.g., carbonic anhydrase,[25] vancomycin,[26] and SH3 domain[27]), is thus not useful here. We derive a form of analysis (different from Scatchard analysis) in which there is no assumption regarding coopera-tivity: for all types of cooperativity (positive, negative, none), this analysis yields a line from which we extract dissociation constants.

As with many affinity experiments, we measure degree of complexation as a function of the concentration of ligand; analysis of these data yields dissociation constants. Our analysis requires that we determine the mobility of the complex of protein bound to ligand *experimentally*: in Scatchard analysis, fully saturating conditions of ligand need never be used experimentally. In a later section, we discuss the potential error introduced into the dissociation constants as a function of the experimental uncertainty in the mobility of the Ig complexed to two ligands. If the value for a dissociation constant is micromolar or less, we can achieve conditions experimentally that make this error acceptably small (10–20%).

(19) Bushey, M. M.; Jorgenson, J. W. *J. Chromatogr.* **1989**, *480*, 301–310.

(20) Chu, Y. J.; Avila, L. Z.; Gao, J.; Whitesides, G. M. *Acc. Chem. Res.*, submitted for publication.

(21) Gomez, F. A.; Avila, L. Z.; Chu, Y.; Whitesides, G. M. *Anal. Chem.* **1994**, *66*, 1785–1791.

(22) Lancet, D.; I. Pecht *Biochemistry* **1977**, *16*, 5150–5157.

(23) Zidovetzki, A. L.; Pecht, I. *Proc. Natl. Acad. Sci. U.S.A.* **1979**, *76*, 5848–5852.

(24) Zidovetzki, R.; Light, A.; Pecht, I. *Mol. Immunol.* **1981**, *18*, 491–497.

(25) Avila, L. Z.; Chu, Y.; Blossey, E. C.; Whitesides, G. M. *J. Med. Chem.* **1993**, *36*, 126–133.

(26) Chu, Y.; Whitesides, G. M. *J. Org. Chem.* **1992**, *57*, 3524–3525.

(27) Gomez, F. A.; Chen, J. K.; Tanaka, A.; Schreiber, S. L.; Whitesides, G. M. *J. Org. Chem.* **1994**, *59*, 2885–2886.

Figure 1. Equilibria involved in Ig–antigen interactions. K_1 is the dissociation constant between the singly occupied Ig and the unoc-cupied Ig. K_2 is the dissociation constant between the doubly occupied Ig and the singly occupied Ig. We denote the degree of cooperativity between K_1 and K_2 as α. Antibodies that bind DNP do so mainly through interaction with the light chain; the binding site is represented as localized on this chain.

DERIVATION OF ANALYSIS

We define two dissociation constants, K_1 and K_2, for the complex between Ig and two ligands (Figure 1).[18,28] The total mobility, μ^{total}, of a molecule, X, is a sum of the mobility due to electroosmotic (EO) flow, μ^{EO}, and the mobility due to electro-phoretic flow, $\mu^{electro}$. Total mobility is inversely proportional, with proportionality constant C_t, to the total time of appearance, t_{app}, that X takes to move from the injection port to the detector (eq 2). We calculate $\mu^{electro}$ by subtracting the EO mobility of the

$$\mu^{total} = \mu^{EO} + \mu^{electro} = C_t/t_{app,X} \qquad (2)$$

neutral marker (in our case, mesityl oxide, MO), μ^{EO}, from μ^{total} (eq 3). ACE relates the changes in $\mu^{electro}$ of a receptor (Ig) on

$$\mu^{electro} = \mu^{total} - \mu^{EO} = C_t\left(\frac{1}{t_{app,X}}\right) - C_t\left(\frac{1}{t_{app,MO}}\right) \qquad (3)$$

complexation with a ligand (L) present in the electrophoresis buffer to the dissociation constant (K_d). When the concentration of ligand is zero, $\mu^{electro}$ is that of free Ig, μ_{Ig}. When the concentration of ligand is sufficiently high that both of the binding sites of the Ig are occupied, the electrophoretic mobility is μ_{IgL_2}. When intermediate concentrations of ligand are present, bivalent Ig receptors exist in three forms: unoccupied (Ig), singly occupied (IgL), and doubly occupied (IgL$_2$). In the present system, we assume (and infer from the line widths of the peaks) that the rates of dissociation (k_{off}) are sufficiently fast (>0.1 s^{-1}) that we observe

(28) Bunting, J. R.; Cathou, R. E. *J. Mol. Biol.* **1973**, *77*, 223–235.

a concentration-weighted average electrophoretic mobility for all three species (we only see one peak at all concentrations of ligand).[29] If we define the total concentration of all forms of Ig as $[Ig_0]$, then the fraction of Ab in form "i" is θ_i.[30] The electrophoretic mobility, $\mu^{electro}$, is the weighted mobility of all three species of Ig (eq 4). The θ_i can be rewritten in terms of K_1, K_2, and $[L]$ by

$$\mu^{electro} = \frac{[Ig]}{[Ig_0]}\mu_{Ig} + \frac{[IgL]}{[Ig_0]}\mu_{IgL} + \frac{[IgL_2]}{[Ig_0]}\mu_{IgL_2} \quad (4)$$

using the definitions from Figure 1. The results are shown in eqs 5–7 and are similar to the equations derived for the

$$\theta_{Ig} = 1\Big/\left(\frac{[L]^2}{K_1K_2} + \frac{[L]}{K_1} + 1\right) \quad (5)$$

$$\theta_{IgL} = 1\Big/\left(\frac{[L]}{K_2} + \frac{K_1}{[L]} + 1\right) \quad (6)$$

$$\theta_{IgL_2} = 1\Big/\left(\frac{K_1K_2}{[L]^2} + \frac{K_2}{[L]} + 1\right) \quad (7)$$

dissociation of a diacid.[30]

The charge on the protein with n ligands, $Z_{P(L)_n}$, is the sum of all charges on the amino acid residues of the protein and all tightly bound species (cofactors, coenzymes, ligands). Z_P is the charge on the uncomplexed protein; Z_L is the charge on the ligand. The electrophoretic mobility of the Ig, μ_{Ig}, is approximately proportional to Z_P and inversely proportional to its hydrodynamic drag with a proportionality constant $C_{\mu,Ig}$. This drag is often set proportional to M^α (eq 8); this equation fits the experimental data relating

$$\mu_{Ig} = C_{\mu,Ig}(Z_P/M^\alpha) \quad (8)$$

electrophoretic mobility to mass for a number of globular proteins.[31,32] The binding of one or two ligands, each with mass m ($\ll M$), and charge Z_L, gives species having electrophoretic mobilities given by eqs 9 and 10, respectively. The proportionality

$$\mu_{IgL} = C_{\mu,IgL}\frac{Z_{P(L)}}{(M+m)^\alpha} = C_{\mu,IgL}\frac{Z_P + Z_L}{(M+m)^\alpha} \cong (Z_P + Z_L)\frac{C_\mu}{M^\alpha} \quad (9)$$

$$\mu_{IgL_2} = C_{\mu,IgL_2}\frac{Z_{P(L)_2}}{(M+2m)^\alpha} = C_{\mu,IgL_2}\frac{Z_P + 2Z_L}{(M+2m)^\alpha} \cong$$

$$(Z_P + 2Z_L)\frac{C_\mu}{M^\alpha} \quad (10)$$

constant C_μ is related to, but not the same as, C_t from eq 2. The

Figure 2. Electrophoretic mobilities of the various protein and protein–ligand complexes.

Charge on complex, $Z_{P(L)_n}$	Z_P	$Z_P + Z_L$	$Z_P + 2Z_L$
Approximate Mass	M	M	M
Electrophoretic Mobility	μ_{Ig}	μ_{IgL}	μ_{IgL_2}
Determined:	experimentally at [L] = 0	using eq 16	experimentally asymptotically at high [L] ([L] > 30K_2)

numerical values of C_μ, $C_{\mu,Ig}$, $C_{\mu,IgL}$, and C_{μ,IgL_2} are not important in this study because they all cancel in the final analysis.

The value for α is $\sim^2/_3$ for small proteins.[31,32] The exact value of α in this work is not important since we assume that M^α will be a constant so long as the bound ligand contributes negligibly to the hydrodynamic drag of its complex with Ig (that is, if m and $2m \ll M$). If, in addition, $C_{\mu,Ig} = C_{\mu,IgL} = C_{\mu,IgL_2} = C_\mu$, then the change in the mobility of the Ig on binding one ligand ($\mu_{IgL} - \mu_{Ig}$) is half the change in mobility on binding two ligands ($\mu_{IgL_2} - \mu_{Ig}$) (Figure 2). Equations 4–10 can be combined and rearranged to give eq 11. Plotting the left-hand side of eq 11 against the

$$\frac{\mu^{electro} - {}^1/_2(\mu_{IgL_2} + \mu_{Ig})}{\mu^{electro} - \mu_{Ig}}[L] = \left(\frac{\mu_{IgL_2} - \mu^{electro}}{\mu^{electro} - \mu_{Ig}}[L]^2\right)\frac{1}{K_2} - K_1 \quad (11)$$

coefficient of the term $1/K_2$ gives a line with slope equal to $1/K_2$ and y intercept equal to $-K_1$.

As [L] increases, $\mu^{electro}$ asymptotically approaches μ_{IgL_2} (Figures 2 and 3). Experimentally, we expect that when increasing [L] does not *observably* increase the value of $\mu^{electro}$, then we have reached $\mu^{electro} \approx \mu_{IgL_2}$. In order to estimate how close our observed electrophoretic mobility is to μ_{IgL_2}, we perform the following iterative experiment: We use some arbitrary value of (or best guess for) the maximum concentration of ligand, $[L]^{max}$. We calculate dissociation constants K_1 and K_2 based on these data using eq 11. We then ask if $[L]^{max} > 30K_2$. If $[L] > 30K_2$, greater than 97% of the Ig is bound to two ligands (and therefore we are very close to μ_{IgL_2}). If $[L]^{max} < 30K_2$, then we collect more data using higher [L] and repeat the analysis using eq 11. We iterate until $[L]^{max} > 30K_2$. This procedure guarantees that we are within $\sim$3% of the actual value of μ_{IgL_2}.[33] A 3% error in μ_{IgL_2} translates into a maximum error of 5% in K_1 and 10% in K_2. There are, of course, other sources of error that further increase the uncertainty in K_1 and K_2; some of these are discussed in more detail in a later section.

(29) If the time for a single dissociation event is, on average, much *shorter* than the time by which the two peaks due to two species are separated, we expect to observe an *average* weighted peak. If this time for dissociation is much *longer* than the time of separation, then we expect to observe *two* individual peaks. If the dissociation rate is intermediate in magnitude, then we expect to observe a broad single peak; we expect this peak to be especially broad at $[L] = K_d$.

(30) Connors, K. A. *Binding Constants: The Measurement of Molecular Complex Stability*; John Wiley & Sons, New York, 1987.

(31) (a) Cantor, C. R.; Schimmel, P. R. *Biophysical Chemistry*; W. H. Freeman: New York, 1980. (b) The application of Henry's equation to proteins yields that the $\mu^{electro}$ becomes independent of mass. Whether or not $\mu^{electro}$ is inversely dependent on mass or independent of mass, however, has little impact on the current work.

(32) Grossman, P. D.; Colburn, J. C. *Capillary Electrophoresis: Theory and Practice*; Academic Press, Inc.: San Diego, CA, 1992.

(33) Achieving the condition $[L]^{max} > 30K_2$ is not possible if this concentration either exceeds the solubility of the ligand in the buffer or significantly changes M^α, C_μ, or C_t.
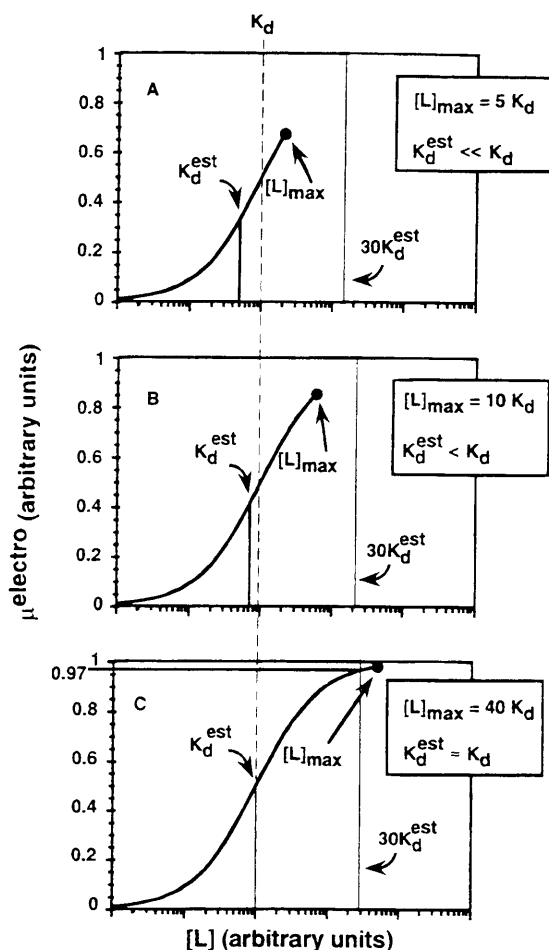
Figure 3. [L] vs $\mu^{electro}$. (A) The highest experimental value of $[L]^{max}$ is much less than $30K_2$ and not sufficiently high to give a reliable value of μ_{IgL_2}. (B) The value of $[L]^{max}$ is less than $30K_2$ and is still not sufficiently high to give a reliable value of μ_{IgL_2}. (C) The value of $[L]^{max}$ is greater than $30K_2$ and is suffiently high that the Ig is within 3% of complete saturation (i.e., $\theta_{IgL_2} \geq 0.97$; eq 5). The error in the estimate of μ_{IgL_2} is less than 3%.

In the case of noncooperative binding, K_d is the dissociation constant for one site and is related to K_1 and K_2 according to eq 12 (Figure 1). A Scatchard plot (eq 13), yields straight lines in

$$K_d = 2K_1 = {}^1/_2K_2 \tag{12}$$

$$\frac{\mu^{electro} - \mu_{Ig}}{[L]} = -K_d^{-1}(\mu^{electro} - \mu_{Ig}) + K_d^{-1}(\mu_{IgL_2} - \mu_{Ig}) \tag{13}$$

$$\Delta\mu = \mu^{electro} - \mu_{Ig} = \frac{\mu_{IgL_2} - \mu_{Ig}}{1 + (K_d/10^{\log[L]})} \tag{14}$$

cases of noncooperative binding (rearranging eq 13 gives eq 14; plotting $\Delta\mu$ against log [L] gives a regular sigmoid). In all other cases (positively or negatively cooperative binding), Scatchard plots are curved. As it is difficult to detect curves by eye, we advocate plotting the data using eq 11 in *all* cases where cooperativity is in question.

The uncertainties in values for K_2 and K_1 are less than 10 and 20%, respectively. For each of the experimental quantities (observables) in our experiment ([L], $\mu^{electro}$, μ_{Ig}, μ_{IgL_2}), there is an uncertainty in its value ($\sigma_{[L]}$, $\sigma_{\mu^{electro}}$, $\sigma_{\mu_{Ig}}$, and $\sigma_{\mu_{IgL_2}}$, respectively).

In our analysis (eq 11), we use these experimental quantities to calculate and plot a pair of points (X, Y), where Y is the left-hand side of eq 11 and X is the coefficient of the term $1/K_2$. The experimental uncertainties in the observables gives rise to uncertainties in X and Y: σ_X and σ_Y.[37] The mathematical relationship between X (or Y) and the observables determines how strongly uncertainties in the observables influence σ_X (or σ_Y). In eq 11, for example, the X value depends on $[L]^2$ and the $\sigma_X^{[L]}$ increases with increasing [L] and $\sigma_{[L]}$ (eq 15). Thus we expect

$$\sigma_X^{[L]} = 2[L]\sigma_{[L]} \tag{15}$$

that data obtained using high concentrations of ligand will display greater scatter than those derived from low concentrations of ligand (this expectation is consistent with our observations shown in Figure 7). This expectation is different when Scatchard analysis is used. In Scatchard analysis, the Y value, Y^{Scat}, is $\Delta\mu/[L]$ (eq 13). The error in Y^{Scat} that is due to uncertainty in [L], $\sigma_{Y^{Scat}}^{[L]}$, decreases rapidly with [L] and increases with $\sigma_{[L]}$ (eq 16). In

$$\sigma_{Y^{Scat}}^{[L]} = \sigma_{[L]}/[L]^2 \tag{16}$$

Scatchard analysis, we expect more scatter in data derived from low concentrations of ligand; one therefore should take more data points from *high* concentrations of ligand. With our analysis, one should, in contrast, use more data from *low* concentrations of ligand (as discussed earlier in Figure 3, we also need to collect several data from *very* high concentrations of ligand to determine μ_{IgL_2} reliably).

The portion of the uncertainty in the X value that is due to $\sigma_{\mu_{IgL_2}}$, $\sigma_X^{\mu_{IgL_2}}$, is given in eq 17. The portion of the uncertainty in Y that is due to μ_{IgL_2}, $\sigma_Y^{\mu_{IgL_2}}$, is given in eq 18.

$$\sigma_X^{\mu_{IgL_2}} = \sigma_{\mu_{IgL_2}}[L]^2\left(\frac{1}{\mu^{obs} - \mu_{Ig}}\right) \tag{17}$$

$$\sigma_Y^{\mu_{IgL_2}} = \sigma_{\mu_{IgL_2}}\left(\frac{[L]}{2(\mu^{obs} - \mu_{Ig})}\right) \tag{18}$$

There are also uncertainties in the plotted data introduced by $\sigma_{\mu^{electro}}$, $\sigma_{\mu_{Ig}}$, and $\sigma_{\mu_{IgL_2}}$. These uncertainties were calculated by mathematically propagating reasonable values for $\sigma_{[L]}$, $\sigma_{\mu^{electro}}$, $\sigma_{\mu_{Ig}}$, and $\sigma_{\mu_{IgL_2}}$. We conclude that the *total* uncertainties in the slope $(1/K_2)$ and Y intercept $(-K_1)$ are, in our experiments and analysis, approximately 5–10 and 15–20%, respectively.

EXPERIMENTAL SECTION

Materials. Rat monoclonal anti-dinitrophenol antibody (Zymed, Clone LO-DNP-11, 1994 Catalog No. 04-8500, purchased in 10 mM phosphate-buffered saline (PBS) at 0.6 mg/mL) was used after ultracentrifugal filtration (molecular weight cutoff 10 000) and lyophilization. Bovine carbonic anhydrase (CA; EC 4.2.1.1, containing CAA and CAB isozymes, from bovine erythrocytes), bovine α-lactalbumin (LA; type I, from bovine milk), the tripeptide Arg-Gly-Asp (RGD), **2**, and mesityl oxide (MO) were purchased from Sigma Chemical Co. and used without further purification. All solutions containing protein were prepared by dissolving

Scheme 1. Synthesis of Ligands 2–5[a]
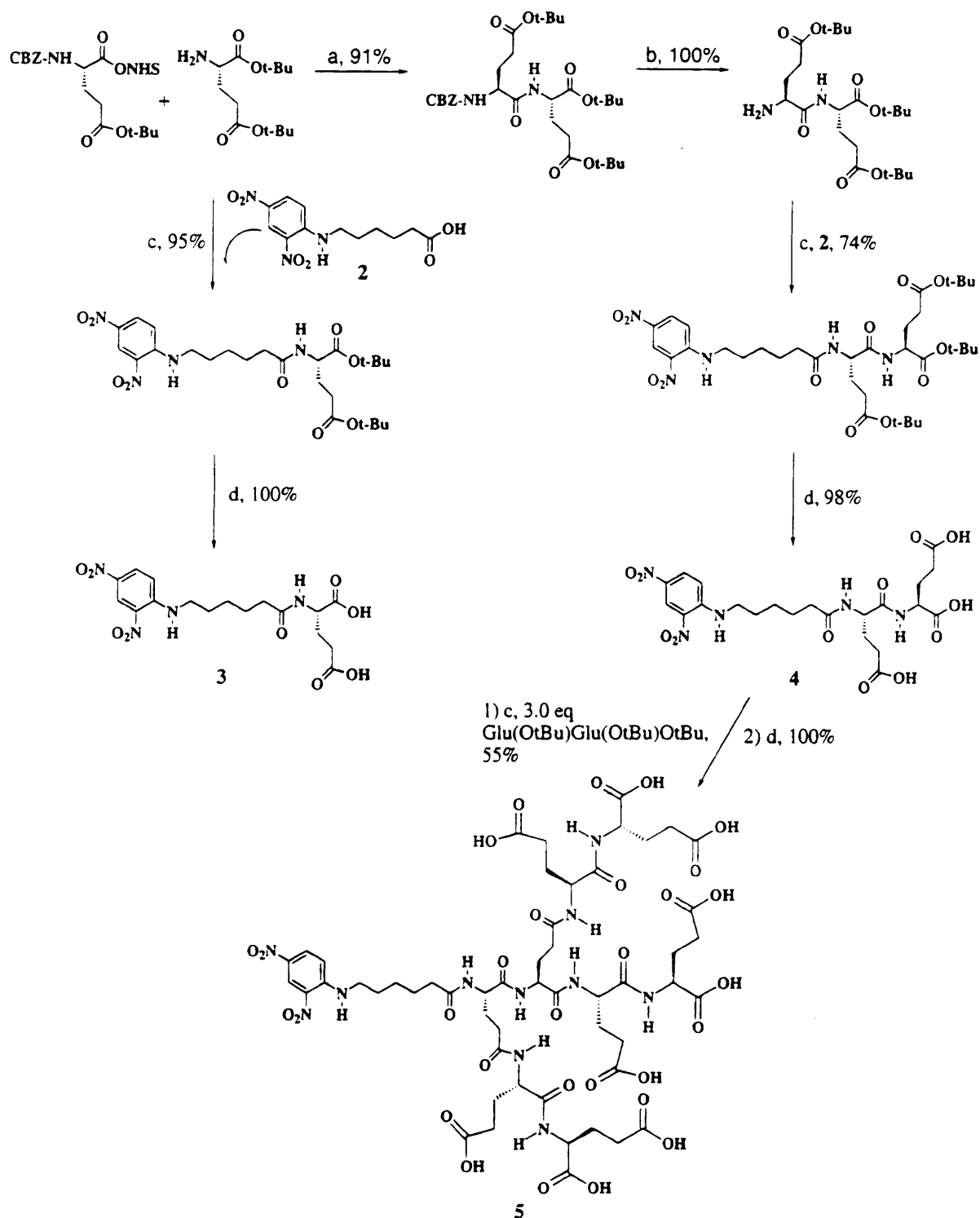
[a] Reagent: (a) CH₂Cl₂; (b) H₂, 10% activated Pd on carbon; (c) dicyclohexylcarbodiimide (DCC), hydroxybenzotriazole (HOBT), and diisopropylethylamine (DIPEA) in dimethylformamide (DMF); (d) trifluoroacetic acid (TFA)–CH₂Cl₂ 1:1.

lyophilized protein into buffer. Organic reagents used in thesyntheses of 1–5 were purchased from Aldrich and used without purification. Reaction solvents were distilled from an appropriate drying agent before use. Reaction mixtures were stirred magnetically and monitored by thin-layer chromatography on silica gel precoated glass plates (Merck). Flash column chromatography was carried out at medium pressure on silica gel 60$_{F254}$ (230–400 mesh, E. Merck) using the solvents that are indicated. Compound 1 was synthesized as previously described.[21] The procedures for

synthesizing and characterizing compounds 2–5 and all intermediates are available as supporting information.
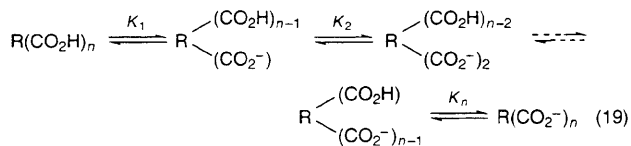
Equipment. Proton and carbon NMR spectra were measured on a Bruker AM-400 MHz NMR spectrometer. Chemical shifts are reported in ppm relative to TMS for the proton spectra and relative to dmso-d_6 at 39.5 ppm for the carbon spectra. The analysis of dissociation constants was performed using an ISCO Model 3140 CE system. The titration of ligands 4 and 5 was performed using a Beckman P/ACE System 5010. The capillary

tubing (Polymicro Technologies, Phoenix) was of uncoated fused silica with an internal diameter of 50 μm, a total length of 57 cm, and a length from inlet to detector of 47 cm.

Procedure for CE. The sample for injection into the electrophoresis capillary consisted of the Ig (0.6 mg/mL), 20 μM mesityl oxide (MO), carbonic anhydrase (CA, 1 mg/mL), α-lactalbumin (LA, 1 mg/mL), and RGD (1 mg/mL). The sample solution ($\sim$8 nL) was introduced into the capillary by vacuum injection. The conditions used during each CE experiment were as follows: voltage, 30 kV; current uncontrolled, but generally 20 μA; buffer, 25 mM Tris-HCl, 192 mM glycine (pH 8.3), 0.5 M **1**, 10 mM K$_2$SO$_4$; detection, 200 nm; temperature 25 $\pm$ 2 °C.
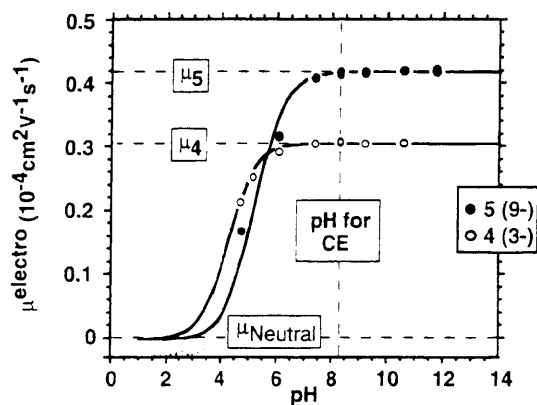
RESULTS AND DISCUSSION

Scheme 1 summarizes the syntheses of DNP analogs **3–5**. We expected that, at pH 8.3, the charges on **2–5** would be -1, -2, -3, and -9, respectively. We validated this expectation for ligands **4** and **5** by monitoring the electrophoretic mobility of these ligands as a function of pH;[34] that is, we titrated the ligands using electrophoretic mobilities as the experimental variable being monitored. The charges on ligands **4** and **5** remain constant at pH >7; all carboxylic acids in these molecules are fully deprotonated at pH >7 (Figure 4). The titration curves fit the theoretical equations[35] that are derived for polyacids in which the values of pK_a for each acidic residue are *independent* of one another, and identical. K_a is the microscopic dissociation constant for one acidic residue (its value may change with different buffers and different ionic strengths). For a polyacid with n independent sites (eq 19), each with microscopic dissociation constant K_a, the molecular dissociation constants, K_m, are defined according to eq 20. The

$$R(CO_2H)_n \xrightleftharpoons{K_1} R\diagdown\diagup\begin{matrix}(CO_2H)_{n-1}\\(CO_2^-)\end{matrix} \xrightleftharpoons{K_2} R\diagdown\diagup\begin{matrix}(CO_2H)_{n-2}\\(CO_2^-)_2\end{matrix} \cdots$$

$$R\diagdown\diagup\begin{matrix}(CO_2H)\\(CO_2^-)_{n-1}\end{matrix} \xrightleftharpoons{K_n} R(CO_2^-)_n \quad (19)$$

$$K_m = \frac{n - (m - 1)}{m} K_a \qquad m = 1 - n \qquad (20)$$

statistical distribution of dissociation constants for the nonaacid molecule, **5**, is $9K_a$, $4K_a$, $(7/3)K_a$, $(3/2)K_a$, K_a, $(2/3)K_a$, $(3/7)K_a$, $(1/4)K_a$, and $(1/9)K_a$; for the triacid **4**, the distribution is $3K_a$, K_a, and $(1/3)K_a$. The theoretical titration curves[35] derived using these statistics fit the experimental mobilities relatively well when the values of the two microscopic dissociation constants are 4.1 and 5.6 for **4** and **5**, respectively. In the present study, we have insufficient data to determine whether the polyacids are truly statistical in their ionization; we suspect that they are not.

We used MO as an indicator of EO flow in these experiments, and CAB, CA, and LA as charged noninteracting (ostensibly) reference materials. These reference materials represent a range of molecular surfaces (uncharged to highly charged) and molecular masses (0.40–30 kDa). Any large systematic change in the mobilities of these species with changing [L] would suggest potential problems with the experiment. For example, if the mobilities of any of the reference materials varied as a function

(34) Cleveland, J. A.; Benko, M. H.; Gluck, S. J.; Walbroehl, Y. M. *J Chromatogr.* **1993**, *652*, 301–308.

(35) We use a manual interative procedure to arrive at the fit shown.

Figure 4. pH vs $\mu^{electro}$. The value of $\mu^{electro}$ of ligands **4** and **5** are measured as a function of the pH of the phosphate buffer (from pH 4.69 to 11.76) using CE (see Experimental Section for exact details). The $\mu^{electro}$ of **4** (●) and **5** (○) are approximately constant at pH >7; all carboxylic acids in these ligands are fully deprotonated at pH >7. The curves drawn through the data represent theoretical titration curves for polyacids in which there are no interactions between acidic groups: the microscopic values for pK_a for **4** and **5** are assigned values of 4.1 and 5.6, respectively. These curves are guides to the eye—they demonstrate only that the data can be fit to a single microscopic pK_a, not that only a single microscopic pK_a is involved.
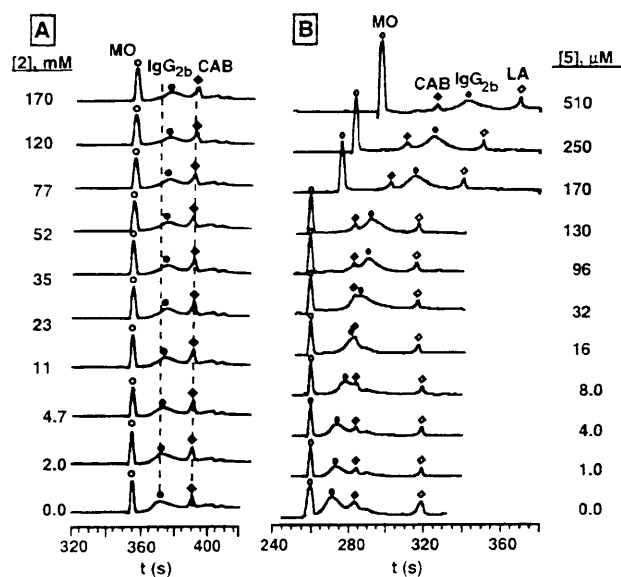

Figure 5. MO as an indicator of rate of EO flow, and CAB and LA as internal references. ACE of IgG$_{2b}$ (see Experimental Section for exact conditions): (A) increasing [2], with charge -1; (B) increasing [5], with charge -9.

of [L], we might have concluded that these materials interacted with the charged ligand.

Figure 5 shows a representative series of electropherograms of Ig in buffer containing various concentrations of **2** and **5**. As expected, the more negatively charged ligand **5** shifts the antibody by a larger amount than the less negatively charged ligand **2**. The broadness of the peak due to Ig may be due to its heterogeneity (possibly due to different states of glycosylation). Figure 6A shows the change in electrophoretic mobilities of Ig, CA, and LA on increasing the concentration of **5**. The approximately horizontal lines for LA and CA indicate that **5** has no affinity for these species. Figure 6B shows the electrophoretic mobility as a function of log [5]. Using the values of values for K_1 and K_2 derived later, and eqs 6–10 and
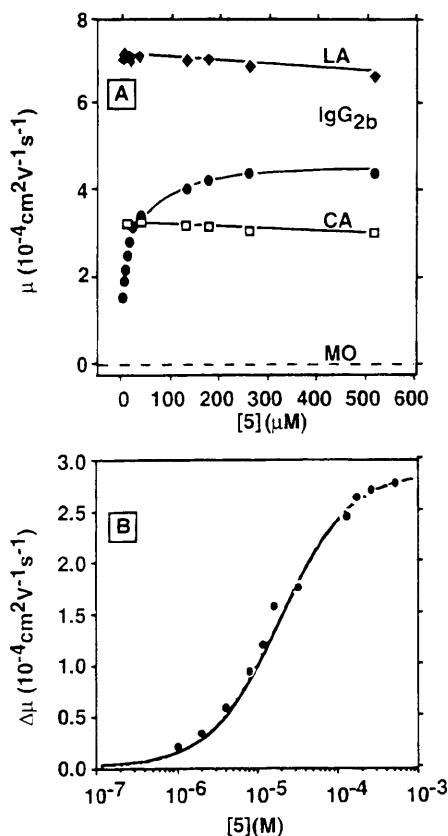
Figure 6. (A) The μ^{electro} of IgG$_{2b}$,MO, LA, and CAB for increasing concentration of **5** (see Experimental Section for exact conditions). The electrophoretic mobility of MO is defined as zero. (B) Change in the electrophoretic mobility of IgG$_{2b}$, plotted against log [**5**]. The sigmoidal curve drawn through the data represent the theoretical fit, assuming that the binding sites are independent (eq 14) and that the microscopic dissociation contant $K_d = 20 \ \mu M$ ($K_1 = 10 \ \mu M$ and $K_2 = 40 \ \mu M$; Table 1).

19, we *calculate* the observed electrophoretic mobility as a function of log [**5**]; the calculated curve fits the experimental data.

In addition to the iterative procedure illustrated in Figure 3, a further check to the experimental value of μ_{IgL_2} is possible in the case where analysis using eq 11 is consistent with noncooperative binding: we plot the data using eq 13. The X intercept yields a value for μ_{IgL_2}. The experimental values of μ_{IgL_2} (obtained from high concentrations of ligand) were within 3% of the value calculated using eq 11.

Figure 7 is a plot of the data from Figure 5 based on eq 11. Table 1 gives the values for K_1 and K_2 that describe the interactions between charged ligands **2–5** and IgG$_{2b}$. Experiments in 0.2, 0.5, and 1.0 M **1** all yielded the same values of K_1 and K_2 (although we can make no more general statement concerning the dependence of dissociation constants on zwitterions).[36]

As is consistent with noncooperative binding, all our systems yield a ratio of K_2/K_1 of ~ 4 (Figure 1). We conclude that binding of monovalent ligands **2–5** to IgG$_{2b}$ is noncooperative.

Defining Charge: $Z_{P(L)_n}$, Z_{exp}, Z_{calc}, Z_{eff}. The charge on a protein can be a theoretical construct, a calculated value, or an experimentally determined value. We define $Z_{P(L)_n}$ as the sum of all charges on the amino acid residues of a protein, P, plus all charges on *tightly* associated molecules including ligands (L), cofactors, and coenzymes (Figure 8). The charges on L and the

(36) Cordova, E.; Gomez, F. A.; Whitesides, G. M., in progress.
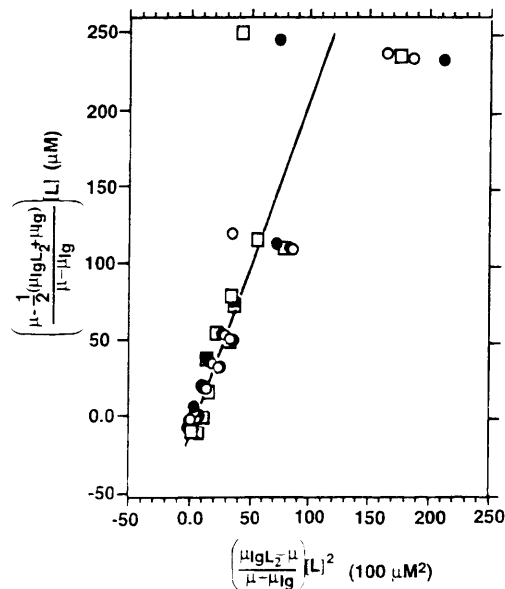
Figure 7. Binding of **5** to IgG$_{2b}$ using eq 11. The plot yields a straight line from which one obtains dissociation constants K_1 and K_2. The data include duplicate trials for three different days (different sample and buffer preparations).

charge on P that is uncomplexed to L are, analogously, Z_L and Z_P, respectively.

The *effective* charge on a protein, Z_{eff}, is treated as a perturbation on Z_P and is an experimental parameter that describes the response of the protein to an electrical field. If the protein is in a solution containing ions, Z_{eff} tacitly *includes* the charges of the ions in the Stern–Helmholtz layer[38] (the stationary boundary layer) surrounding the protein (Figure 8). Z_{eff} is in general (but need not necessarily be) lower than Z_P (as a result of "charge shielding"). The relationship between Z_P and Z_{eff} is given by eq 21. The term q (eq 21) reflects the degree of shielding of Z_P by

$$Z_{eff} = Z_P/(1+q) \qquad (21)$$

ions in solution and is approximately proportional to the ionic strength of the solution: if $q \ll 1$, then shielding is negligible.

The μ^{electro} is linearly proportional to Z_{eff} (eq 22). Using eq 21,

$$\mu^{\text{electro}} = C_\mu^{\text{eff}} \frac{Z_{eff}}{M^\alpha} = \frac{C_\mu^{\text{eff}}}{(1+q)} \frac{Z_P}{M^\alpha} = C_\mu \frac{Z_P}{M^\alpha} \qquad (22)$$

μ^{electro} is also linearly proportional to Z_P (eq 22). The proportionality constants that relate Z_P and Z_{eff} to μ^{electro} are C_μ and C_μ^{eff}, respectively; C_μ and C_μ^{eff} are consequently related by eq 23.

$$C_\mu = C_\mu^{\text{eff}}/(1+q) \qquad (23)$$

We use CE to estimate *experimentally* the charge on a protein, Z_{exp}, from the mobilities of a protein and its complexes with differently charged ligands (described in detail

(37) In general, if X is a function of the two experimental observables a and b ($X = f(a,b)$), then $(\sigma_X)^2 = (\sigma_X^a)^2 + (\sigma_X^b)^2 = (\partial X/\partial a)^2(\sigma_a)^2 + (\partial X/\partial b)^2(\sigma_b)^2$: Skoog, D. A. *Principles of Instrumental Analysis*; Saunders College Publishing: Fort Worth, TX, 1985; pp 5–22.

(38) Knox, J. H. *J. Chromatogr.* **1994**, *680*, 3–13.

Table 1. Dissociation Constants of the IgG2b Complexes with Ligands 2–5[a]

ligand	charge[b]	K_1^c (μM)	K_2^d (μM)	K_2/K_1
2	−1	1.9 ± 0.4	8.5 ± 0.9	4.5 ± 0.9
3	−2	2.8 ± 0.6	9.5 ± 1.0	3.4 ± 0.7
4	−3	5.8 ± 1.2	19 ± 1.9	3.3 ± 0.7
5	−9	9.0 ± 1.8	40 ± 4.0	4.4 ± 0.9

[a] 192 mM Tris, 25 mM glycine, 10 mM K_2SO_4, 0.5 M 1. [b] Charge on the ligand in aqueous solution, pH 8.3. [c] Probable error in K_1 is 20%. [d] Probable error in K_2 is 10%.

below). We will show that if the values of q, M, and C_μ^{eff} remain constant for the protein and its complexes, then $Z_{exp} \approx Z_P$ (Figure 8).

We may also *calculate* a charge on the protein from values of pK_a and pH. We refer to this calculated charge on the protein as Z_{calc}. If the values of pK_a and pH are known exactly, then $Z_{calc} \approx Z_P$ (Figure 8).

The experimental charge (Z_{exp}) of this IgG_{2b} is −8.0 at pH 8.3. It has been difficult to estimate the charge, Z_P, on a protein.[39–42] We recently reported a method of inferring the charge, Z_{exp}, *experimentally* for small (MW <50 000) proteins.[42] In that analysis, we acylate the protein partially under nondenaturing conditions to create a family of differently acylated derivatives, that is, a *charge ladder*. Analysis of the electrophoretic mobilities of the differently acylated derivatives yields Z_{exp}. We are, however, unable to use this method for proteins of high molecular weight (MW$_{Ig}$ = 150 000) because we are unable to separate the components of the charge ladder with resolution that is sufficient for analysis.

In this paper, we use the change in electrophoretic mobility of the protein in complexing charged ligands to evaluate Z_{exp}. This method has been used previously to determine the value of Z_{exp} for carbonic anhydrase at various pH values.[42] This method also requires the syntheses of multiple ligands with different values of charge and is therefore less convenient than the method based on charge ladders. It is free of some of the limitations due to the molecular weight of the protein. The electrophoretic mobility of the complex, μ_{IgL_2}, is proportional to the charge of the ligand, Z_L (eqs 9–11). A *ratio* of μ_{IgL_2} to μ_{Ig} is only dependent on the charges of the protein, Z_P, and the ligand, Z_L, *if* the mass, M, and the proportionality constant, C_μ^{eff}, and the correction for effective charge, $(1 + q)$,[43] *all* cancel (eq 24). In general, however, we do

$$\frac{\mu_{IgL_2}}{\mu_{Ig}} \approx \left(\frac{1 + q_P}{1 + q_{P(L)_2}}\right)\left(\frac{M^\alpha}{(M + 2m)^\alpha}\right)\left(\frac{C'_{\mu,P(L)_2}}{C'_{\mu,P}}\right)\frac{Z_P + 2Z_L}{Z_P}$$

$$\cong 1 + \frac{2Z_L}{Z_{exp}} \qquad (24)$$

not know that all these values cancel, and thus we refer to Z_P in eq 24 as Z_{exp} (an experimental *estimate* of Z_P). Rearranging eq

24 yields eq 25. Plotting the left side of eq 25 (corresponding to

$$2Z_L = Z_{exp}((\mu_{IgL_2}/\mu_{Ig}) - 1) \qquad (25)$$

the *total* charge of ligand bound to the protein) against the coefficient of the term Z_{exp} gives a line with a slope equal to Z_{exp}.[44] From the analysis of the data for the binding of Ig to ligands 2–5 by this method, we determine that for Ig (MW 150 000), $Z_{exp} = -8.0 \pm 0.2$ at pH 8.3 (Figure 9); we therefore *estimate* that $Z_P \approx -8.0 \pm 0.2$ at pH 8.3.

The linearity of this plot further indicates that the experimental estimate of μ_{IgL_2} (using very high concentrations of ligand) was acceptably good; if the experimental value of μ_{IgL_2} underestimated its actual value, then the plot would appear curved downward at higher values of $2Z_L$. The linearity also validates $Z_{P(L)} = Z_P + Z_L$; the data point for μ_{Ig} would have deviated from the line if this relation did not hold.

CONCLUSIONS

Use of ACE To Study Interactions of Antibodies with Ligands. Quantifying the interaction between bivalent antibodies and the ligands to which they bind is central to molecular immunology. Enzyme-linked immunosorbent assays (ELISA)[45] radioimmunoassays (RIA)[45] equilibrium dialysis,[46] and immunoprecipitation (the Farr method[47]) are widely used to quantify these interactions. These methods yield a single relative binding constant with a substantial error.[48] Other methods—fluorescence,[49] surface plasmon resonance (SPR),[50] and stopped-flow kinetics[51] —often require modifying the antibody; they are also time-consuming. This study demonstrates that ACE can be used to estimate *both* dissociation constants—regardless of cooperativity—for the interaction of Ig antibodies and monovalent ligands of low molecular weights. The use of Jorgenson buffers[19] gave acceptable (although still broad) line shapes. We believe that although the concentrations of zwitterionic additives in these buffers (500 mM) give solutions of higher ionic strength and viscosity than normally used for biological assays, the results are still relevant to biology. We estimate the ionic strength of the interior of a cell to be between 0.5 and 1.1 M.[52] In addition, the interior of a cell contains a large number and high concentration of organic

(39) Ojteg, G.; Lundahl, P.; Wolgast, M. *Biochim. Biophys. Acta* **1989**, *991*, 317–323.

(40) Nozaki, Y.; Tanford, C. *Methods Enzymol.* **1967**, *11*, 715–734.

(41) Ford, C. L.; Winzor, D. J. *Biochim. Biophys. Acta* **1982**, *703*, 109–112.

(42) Gao, J.; Gomez, F. A.; Harter, R.; Whitesides, G. M. *Proc. Natl. Acad. Sci. U.S.A.* **1994**, *91*, 12027–12030.

(43) The value of q is unknown in this experiment. Theoretically, it is dependent to differing degrees on the characterisics of both the molecule and the solution. The value of q is strongly dependent on the ionic strength of the solution. If all measurements are done in buffer of constant ionic strength, then the assumption that q remains constant for the protein and its complexes may be a good one.

(44) If the relationship between Z_{eff} and Z_P (eq 11) is different for the different L (that is, the values of q_{1g2}, q_{1g3}, q_{1g4}, and q_{1g5} differ), then the measured value of charge using eq 24 will be different from Z_P.

(45) Goldberg, M. E.; Djavadi, O. L. *Curr. Opin. Immunol.* **1993**, *5*, 278–281.

(46) Gopalakrishnan, P. V.; Karush, F. *Immunochemistry* **1974**, *11*, 279–283.

(47) Farr, R. S. *J Infect. Dis.* **1958**, *103*, 329.

(48) The uncertainty in these techniques is not better than a factor of 2–4.

(49) Dandliker, W. B. *Methods Immunol. Immunochem.* **1971**, *3*, 435–453.

(50) Malmqvist, M. *Curr. Opin. Immunol.* **1993**, *5*, 282–286.

(51) Kitano, H.; Hasegawa, J.; Iwai, S.; Okubo, T. *Polym. Bull. (Berlin)* **1986**, *16*, 89–93.

(52) In 1000 g of HeLa cells, there are 10 g of small inorganic ions (MW = 40; 0.25 M); 60 g of small molecules (MW = 400; 0.28 M); 19 g of cytoplasmic RNA (effective molarity ranges from 0 to 0.06 M); 225 g of protein (effective molarity ranges from 0.01 to 0.48 M). The total effective molarity then ranges from 0.53 to 1.07 M. The total concentration of organic molecules is approximately 300 g (30%). Data drawn from: Darnell, J.; Lodish, H.; Baltimore, D. *Molecular Biology*, 2nd ed.; W. H. Freeman and Co.: New York, 1990; pp 114–115.
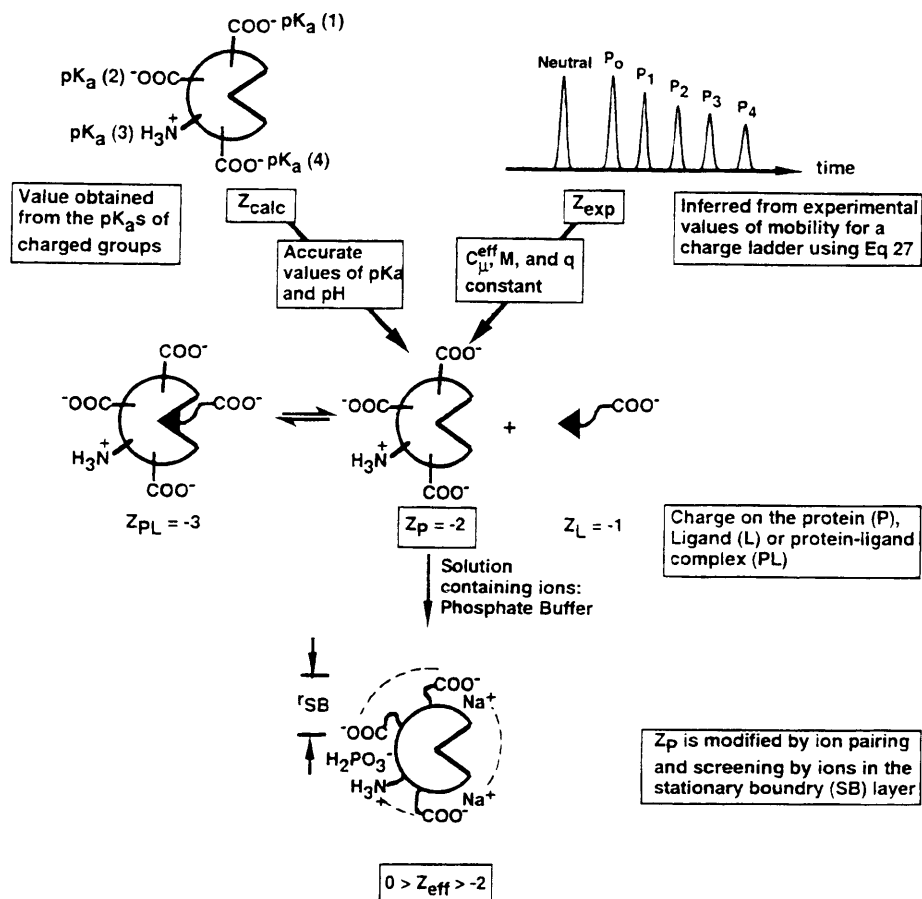
Figure 8. Summary of terms referring to the charge of a protein. $Z_{P(L)_n}$ represents the total charge on the protein plus the charge on all tightly associated ligands, cofactors, and coenzymes. Z_P and Z_L are, analogously, the charges on the uncomplexed protein and the ligand, respectively. In the hypothetical example used here for illustration, $Z_{P(L)_n}$, Z_P, and Z_L are -3, -2 and -1, respectively. The effective charge of the protein, Z_{eff}, is Z_P minus the average net charge of counterions in the stationary boundry layer (Stern–Helmholtz layer) of solvation (represented here by a sphere of radius r_{SB}). The counterions in the stationary boundry layer exchange slowly with the other ions in solution. We do not know the value of r_{SB} in our experiments and therefore, do not know the difference in magnitude between the values of Z_{eff} and Z_P. In the hypothetical example shown here, the net charge of the counterions in the sphere of radius r_{SB} is $+1$ and Z_{eff} is -1. Z_{calc} is the charge on the protein calculated from values of pK_a of the amino acid residues and the value of pH. If the values of pK_a and pH are known exactly, then $Z_{calc} \approx Z_P$. Z_{exp} is the charge on the protein that is inferred from experiment; if the coefficients that relate Z_P to mobility (C_μ^{eff}, M, and q) remain constant, then $Z_{exp} \approx Z_P$.

materials ($\sim$300 g/L[52]). The complex buffers used in this study (having high ionic strength—500 mM—and high concentrations of organic materials—110 g/L), in our opinion, more closely simulate intracellular conditions than do the simple buffers often used for biological assays.

The rate of electroosmotic flow changed substantially on increasing the concentration of ligands (especially **4** and **5**). By using internal standards and mobilities (rather than absolute appearance times, t_{app}), we believe that we have successfully corrected for these changes.[21] We therefore did *not* need to have highly reproducible values of t_{app} in our experiments. The use of internal standards to correct for changes in EO flow is central to the success of these analyses.

Ligands that were highly charged clearly shifted the electrophoretic mobility of the Ig; even, however, a ligand with a *single* charge gave shifts that were detectable and reproducible. The association of a ligand with one unit of charge to the Ig (that is, two units per bivalent Ig) changes the mobility by $\sim$25% since $Z_{exp} \approx -8$. This change is detectable even with the broad lines that we observe. Other Igs will have similar (although not identical) changes. We feel that, in principle, one can quantify the binding of Ig to *any* low molecular weight ligand that is either

naturally charged or contains a site for attaching a charged group; extension of the analysis to ligands large enough that the antibody–ligand complex and the antibody alone have different hydrodynamic drag should be possible, but requires exploration.

Monitoring the electrophoretic mobilities of the *ligands* as a function of the pH of the buffer allowed us to determine the degree of ionization. Such an experiment allows the determination of pK_a in some cases.[34]

Analysis of the Data. The analysis used here is useful (and may be more appropriate than Scatchard analysis) for polyvalent systems in which cooperativity between binding events is in question. There were five assumptions used in this analysis: (i) the mobility of the fully complexed antibody, μ_{IgL_2}, can be estimated experimentally at high values of [L] to within 3% of its value; (ii) binding of the ligands to the protein affected the hydrodynamic drag of the protein negligibly; (iii) the values of k_{on} and k_{off} are sufficiently large that the observed mobility is a concentration-weighted average of the mobilities of all complexes containing Ig; (iv) the proportionality constants $C_{\mu,Ig}$, $C_{\mu,IgL}$, and C_{μ,IgL_2} (eqs 8–10) that relate electrophoretic mobility to mass and charge are equal in magnitude; (v) the hydrodynamic drag (M^c) is constant for Ig and its complexes.
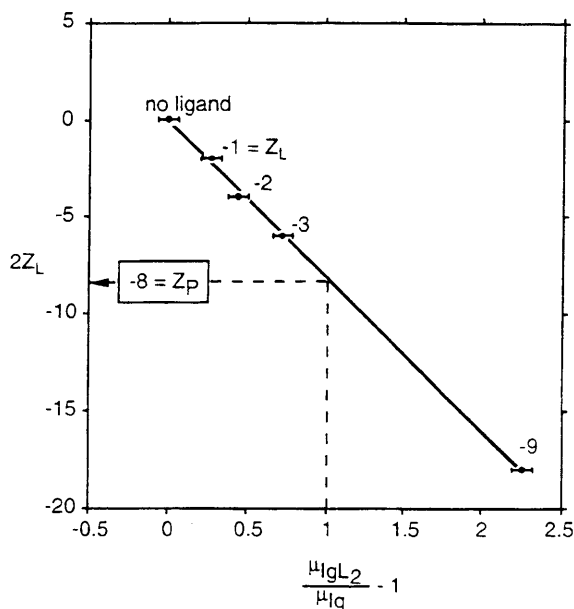
Figure 9. Total charge of the bound ligands, $2Z_L$, against the coefficient of the experimental charge on Ig, Z_{exp} (eq 25). The plot gives a line whose slope yields Z_{exp}. Z_{exp} on IgG$_{2b}$ (MW 150 000) at pH 8.3 is -8.0. The horizontal error bars represent a 3% uncertainty in the X value. When the value of $X = 1$, then $Y = Z_{exp}$ (indicated by a dashed line). The labels on the points of data represent values for Z_L.

Our analysis indicates that the binding of two ligands to this Ig is noncooperative (independent). Noncooperative binding between a bivalent antibody and two small monovalent ligands is intuitively reasonable. Noncooperative binding is less obviously indicated for ligands in which charge—charge interactions might be significant.[53] The previously reported positively cooperative binding between monovalent DNP-containing ligands and an anti-

DNP antibody was rationalized through conformational changes on binding the first ligand.[22-24] Since these groups used different antibodies, we can make no comment on their results.

Use of ACE To Estimate the Charge of an Antibody in Solution. A useful method of estimating the charge, Z_P, on large proteins uses analysis of binding to a family of ligands that differ in charge. This method is based on one used by Gao[42] and yields a value for the experimental charge, Z_{exp}, of a protein in solution at a given pH. The mobilities of Ig and its complexes are linearly related if all other terms in the equation relating mobility to charg—namely, C_μ^{eff}, M, and q—remain constant: Z_{exp} is an *estimate* of Z_P. The method of estimating Z_P using covalent charge ladders is currently most useful for proteins with molecular mass less than 50 kDa; that based on examining relative mobilities of a series of protein—ligand complexes with different charges is more laborious, but is also applicable to higher molecular weight proteins. Neither a crystal structure nor information on the sequence exists for the Ig studied here. Thus, our prediction of the charge for the IgG$_{2b}$ used in this study ($Z_P \approx -8.0$ at pH 8.3) is the first of which we are aware.

SUPPORTING INFORMATION AVAILABLE

Detailed procedures for the synthesis and characterization of compounds 2–5 and all intermediates (5 pages). See any current masthead page for ordering information.

(53) The binding sites in the bivalent antibody are approximately 100 Å apart and one ligand, therefore, is not likely to hinder the binding of the other ligand sterically: Schref, T.; Hiller, R.; Naider, F.; Levitt, M.; Anglister, J. *Biochemistry* **1992**, *31*, 6884–6897